RESILIENT INFRASTRUCTURE
June 1–4, 2016
RESILIENT INFRASTRUCTURE LONDON 2016

OPTICAL TRACKING OF DEBRIS IN EXTREME HYDRODYNAMIC CONDITIONS

Jacob Stolle
University of Ottawa, Canada

Ioan Nistor
University of Ottawa, Canada

Nils Goseberg
Institute for Hydraulic, Estuarine and Coastal Engineering, Leibniz University of Hannover, Germany
University of Ottawa, Canada

ABSTRACT

Debris impact on structures have been reported and shown to be a major reason for structural failure in many post-mortem site assessments of tsunami devastated communities. However, due to the random nature of the debris motion, determining areas at-risk for debris impact is difficult. This paper presents a novel camera-based object tracking algorithm which allows for the quick and accurate tracking of debris trajectory in highly turbulent flows. The algorithm was used to determine debris motion observed during an experimental program on the displacement of scaled-down shipping containers (debris), carried out by the authors in the Tsunami Wave Basin at Waseda University, Tokyo, Japan. This study evaluated the effect of the initial orientation and number of debris on the time histories of their trajectory, orientation and velocity. The study found that, while random in nature, the motion of the debris was highly repeatable through the various tests conducted. An increase in the number of debris resulted in a higher peak debris velocity. Setting the initial orientation of the long-axis of the debris perpendicular to the flow direction resulted in an earlier and higher peak velocity than in the case of the debris initially oriented parallel to the direction of the flow.

Keywords: Debris, Debris Motion, Tsunami, Object Tracking, Impact Force, Coastal Engineering, Physical Modeling

1. INTRODUCTION

The 2011 Tohoku Japan Tsunami was among one of the most tragic and destructive natural disasters, with over 15,500 fatalities and an estimated $209.8 trillion (USD) dollars in damage (Fujii et al., 2011, Kazama and Noda, 2012). The primary reason for the extraordinary scope of the damage was due to the fact that coastal communities and associated infrastructure located within the tsunami inundation area lacked the necessary capacity to handle the extreme hydrodynamic forces (Esteban et al., 2015). As a result, a sustained research effort worldwide focused on identifying the loading conditions occurring in the extreme hydraulic events.

Although Canada has avoided any extreme damage due to tsunamis in recent history, the West Coast of Canada and the United States of America (USA) is vulnerable to tsunamis, generated from earthquakes along the Pacific “Ring of Fire”, nearly as large as the tsunami that struck Japan in 2011 (Clague et al., 2003, Palermo et al., 2009). The increased risk to the West Coast of North America has led the American Society of Civil Engineers (ASCE) to develop a new standard, written in mandatory language, specifically targeting communities at risk of tsunami events (*ASCE 7: Tsunami Loads and Effects, 2016*). While these standards cannot prevent damage from a tsunami, appropriate design and preparedness of at-risk communities can greatly reduce the devastation level of such events (Johnston et al., 2005, Taubenböck et al., 2009, 2013).

Building failure due to debris impact has been reported in some forensic engineering site assessments of tsunami-stricken regions (Figure 1). However, the impact forces and areas at-risk of debris impact are difficult to evaluate

(Yeh et al., 2013). Determining areas at risk of debris impact requires an in-depth understanding of the debris motion as many variables affect their overall motion, such as properties of the debris (i.e. mass and geometry), surrounding environment as well as flow conditions (Matsutomi et al., 2008, Matsutomi, 2009, Naito et al., 2014). For impact loading, which is the variable that determines the design condition of at risk structures, the velocity and orientation of debris on impact are critical properties of the debris motion to consider (Matskevitch, 1997, Haehnel and Daly, 2004, Aghl et al., 2015). The examination of debris motion has been difficult due to the random nature of the process (Matsutomi, 2009). The examination of the motion has been particularly difficult in an experimental setting due to a lack of methods that can quickly, accurately and non-invasively track the motion of the debris. Historically, debris motion has been evaluated by determining the maximum inundation and final resting position of the debris using image-by-image analysis (Imamura et al., 2008, Matsutomi, 2009). However, this method is time-consuming and does not capture the intermediate steps involved in debris motion such as the maximum velocity and orientation. Recently, more sophisticated image processing techniques have been used to evaluate the debris motion (Rueben et al., 2014, Yao et al., 2014) as well as wirelessly equipped debris ("smart" debris) for quicker and more accurate evaluation of debris motion (Shafiei et al., 2014, Goseberg et al., 2015).

Figure 1: Debris impact on structures following the 2011 Tohoku Japan Tsunami (Nistor, 2011).

This paper examines the motion of scaled-down 20-feet shipping containers (debris) on a horizontal bottom using a novel image processing algorithm that quickly and accurately tracks the trajectory and orientation of the debris in high velocity flow. The objectives of this paper is to analyze:

- The repeatability of the debris motion.
- The effect of the initial orientation of the debris on the debris motion under extreme flow conditions.
- The effect of the distance from the initial debris site on the potential impact forces of the debris.

The paper consists of the following sections: the "Experimental Setup" section outlines the test setup at Waseda University, Tokyo, Japan and briefly outlines the necessary equipment. For a more in-depth description of the experimental setup, see Nistor et al. (2016). The "Debris Tracking" section outlines the camera-based debris tracking algorithm that was used in evaluating the debris motion. The algorithm is further described in Stolle et al. (2016). Finally, "Results and Discussion" analyzes the results of the experiments focusing on the debris trajectory and velocity while "Summary and Conclusions" outlines the findings of the paper and the potential next steps in the research.

2. EXPERIMENTAL SETUP

2.1 Tsunami Wave Basin

The experimental program was conducted in the Coastal Engineering and Management Laboratory at the Department of Civil and Environmental Engineering at Waseda University, Tokyo, Japan. For these tests, a newly-constructed Tsunami Wave Basin (TWB) was utilized (Figure 2). The TWB was equipped with a four-chamber overhead reservoir,

fillable with a vacuum pump (TST-150, Sato Vac Inc., Japan). The maximum achievable hydraulic head with reference to still water elevation was 0.77 m. The water impoundment was released through computer-controlled air valves (SVB1V-50F-02HS, CKD Corporation, Japan).

At the opposite end of the wave basin an elevated, rigid horizontal apron, mimicking a harbor environment, was constructed. A vertical quay wall separated the "sea" section of the basin from the dry, horizontal apron. A right-handed coordinate system with the origin at the midpoint of the edge of the quay wall was used throughout the tests. The y-axis was positive in the onshore direction of the wave propagation. The vertical axis was positive in opposite direction of the gravity vector, with z = 0 at the elevation of the apron area. Two high-definition (HD) cameras (Basler AG, pi1900-32gc, Germany) were mounted at the apron's end of the wave basin on an instrument frame positioned at a height of 2.95 m above the apron area and pointing towards the area of interest (AOI).

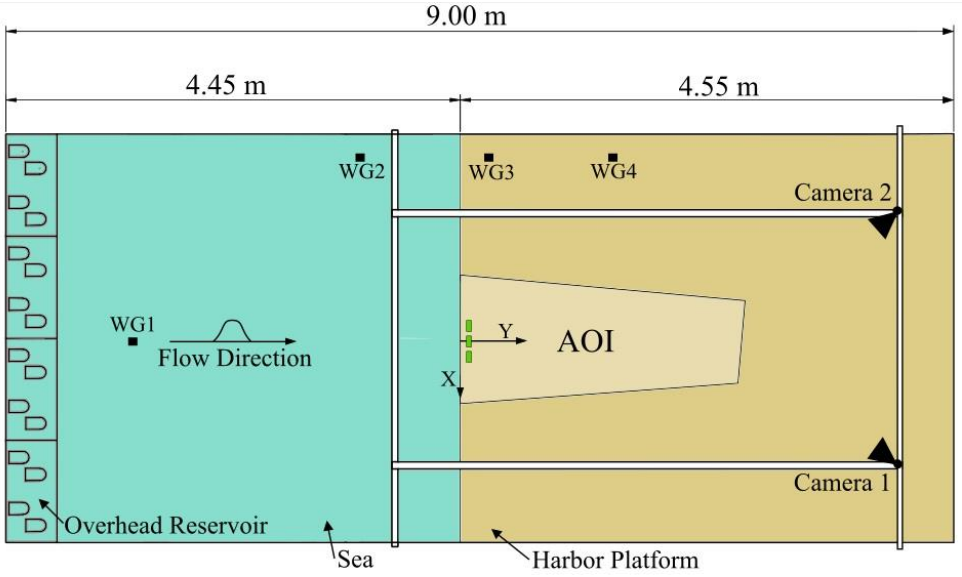

Figure 2: Tsunami Wave Basin (TWB) at Waseda University, Tokyo, Japan.

2.2 Debris Model

The debris consisted of an idealized 20-feet shipping containers (ISO668/688) down-scaled based on Froude similitude at a length scale of 1 in 40. The down-scaled shipping container, shown in Figure 3, were manufactured from positively buoyant polyethylene (PE-HMW, 0.92 g/cm³). The scaled shipping container had overall dimensions of 0.06 x 0.06 x 0.15 m with an approximate draft of 0.025 m. The debris was placed centered on the TWB harbor platform, 0.20 m in the positive y-direction from the vertical quay wall (Figure 2).

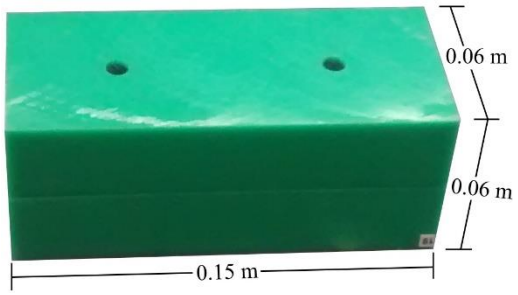

Figure 3: Debris model: scaled-down ISO shipping container (1:40 Froude scale).

2.3 Experimental Test Program

The paper presents the results of 13 of 45 experiments performed in the TWB at Waseda University (Table 1). The experiments comprise the effect of orientation and number of debris on the trajectory and velocity of the debris as the debris passed through the AOI. For each test, the water depth in the TWB was set to 0.235 m in the "sea" section, leaving thus a freeboard of 0.015 m between the harbor still water level and the level of the dry apron area. Before each test, the wave maker vacuum reservoirs were filled with the same volume of water resulting in a hydraulic head of 0.67 m above the harbor's still water level. The filling level of the vacuum chambers was controlled to ensure the same hydraulic conditions of the generated wave. The hydraulic head used in all tests was related to the total amount of water impounded in the reservoir chambers (1.2 m^3 total volume) which was released by the opening of the computer-controlled air valves.

Debris were placed with the centroid of the debris 0.23 m from the edge. For experiments with one debris (E01 and E02), the centroid of the debris (D2) was placed on the y-axis. For experiments with three debris (E03 and E04), the centroid of D2 was placed on the y-axis and the spacing in the x-direction between the centroids of the debris to each side was 0.18 m (0.03 m spacing between the debris). The initial orientation of the debris was either 0^o, where long axis of the debris was placed perpendicular to flow direction, or 90^o, where the long axis of the debris was placed parallel to flow direction.

Table 1: Experimental Test Program

ID	Number of Debris	Initial Debris Orientation [^{o}]	Initial Y-Position [m]	Test ID [#]
E01	1	0	0.23	1, 2, 3, 4, 5
E02	1	90	0.23	6, 7, 8
E03	3	0	0.23	10, 11
E04	3	90	0.23	12, 13, 14

3. DEBRIS TRACKING

A camera-based image processing algorithm was developed for the tracking of multiple uniform debris in high-velocity flow (Stolle et al., 2016). The objective of the algorithm was to quickly and accurately track the debris through the AOI to provide high-quality data of the motion of the debris. The algorithm used raw images recorded by the camera. By using image processing techniques determined the position and orientation of the debris within each frame. The algorithm was validated using a manual image-by-image selection of the debris for selected experiments from the Waseda University experimental program. This section provides a brief outline of the tracking algorithm, but a more detailed explanation can be found in Stolle et al. (2016).

The tests were performed at Waseda University in the Tsunami Wave Basin which is located outdoor. Therefore, the algorithm had to handle a large variety of lighting conditions. The primary method of dealing with this issue was to transform the traditional color space of the raw image (each pixel being expressed as a Red-Green-Blue value) into a three-dimensional luminance-chrominance color space (each pixel being expressed as a Luminance (Y)- Blue Chroma (C_b)- Red Chroma (C_r) value), which has less redundancies associated with the expression of an individual color (Chai and Bouzerdoum, 2000). The new color space allowed the algorithm to track the green color of the debris using the chrominance vales and the shading was expressed in the luminance. Moreover, the image must be transformed from the image plane to the camera plane using *geo-rectification*. Using control points located on the outside edges of the AOI, each pixel in the image could be placed within the coordinate system specified in Figure 2. The rectified image is shown in Figure 4(a).

Within each rectified image, the debris needed to be identified from the image background and water surface. Since the debris was of uniform green color, *color thresholding* (Harrabi and Braiek, 2011) was used to segment the image. *Color thresholding* used a Boolean operation on the three values used to express each pixel ($Y\text{-}C_b\text{-}C_r$) and if each value falls within the specified thresholds the pixel was assigned a "1" (white) or "0" (black). The *color thresholding* resulted in a binary image, as shown in Figure 4(b). An image processing technique, referred to as *blob analysis* (Salvi,

2012), searched the binary image for interconnected "1" pixels large enough to be the debris. *Blob analysis* also provided important geometric feature of the interconnected pixel, such as the centroid and long axis. The centroid was used in determining the trajectory of the debris and the long axis was used to determine the orientation of the debris.

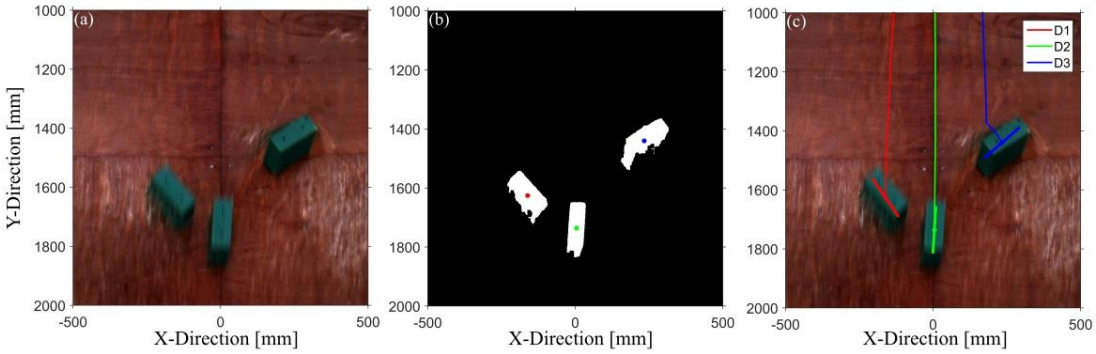

Figure 4: Camera-based optical tracking algorithm used in the tracking of debris (D1 – D3) motion. (a) Raw data frame from the camera; (b) binary image from the color thresholding; and (c) debris tracked using their centroid and orientation.

Based on the above mentioned steps, the debris was identified in each image. However, the information from each image had to be assigned to the unique debris to track it continuously through the AOI. This process was completed using a *Kalman filter* (Laplante and Neill, 2003). Based on the previous motion of the debris, the *Kalman filter* predicts the position of the debris in each image. With both the predicted position of the debris using the *Kalman filter* and the observed position of the debris, employing the *blob analysis*, a matching algorithm (Munkres, 1957) was used to match the observed positions at a given time to the observed positions recorded in the previous frames.

Figure 5 shows an example of the frame-by-frame tracking of video data from the experiments performed in the Tsunami Flume at Waseda University. The algorithm quickly and accurately tracks the trajectory of the debris and the orientation of the debris as it propagates through the area of interest. The algorithm performed well when compared to the manual method, except in cases where significant agglomeration occurred between the debris (Stolle et al., 2016).

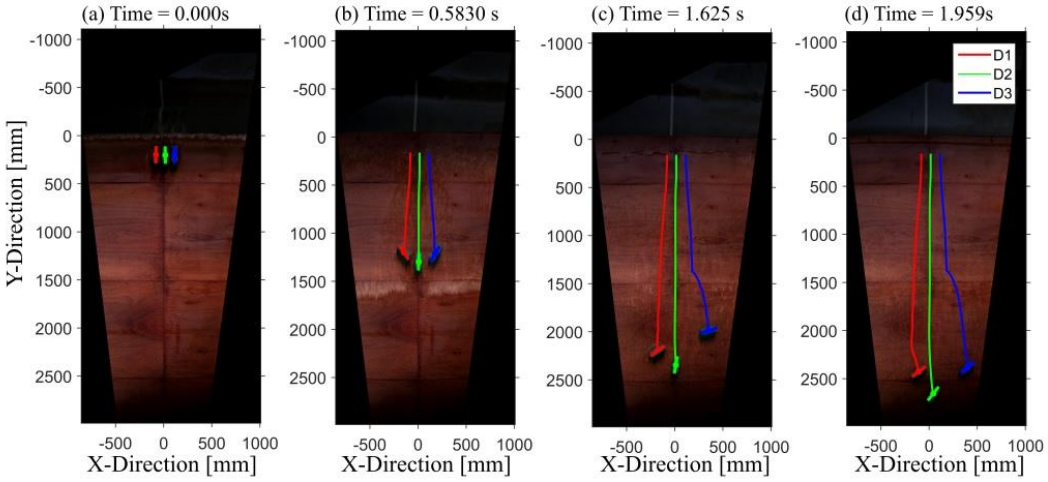

Figure 5: Trajectory of debris (D1 – D3) in experiment #12 (E04) at four instances in time: (a) 0.000 s; (b) 0.5830 s; (c) 1.625 s; (d) 1.959 s.

4. RESULTS AND DISCUSSION

4.1 Hydrodynamics

The wave maker in the TWB impounded a head of 0.655 m in the overhead reservoirs, which was kept constant throughout all tests to maintain comparable hydrodynamics conditions. The water was released from the reservoir and would propagate through the "sea" section as an elongated solitary wave (Nistor et al., 2016). The wave front showed good agreement with the analytical solution for a solitary wave by Munk An elongated tail was generated after the wave front resulting in a longer duration flow compared to the solitary wave definition (Madsen et al., 2008). As the wave approached the vertical quay wall, the wave began to shoal and break, propagating over the horizontal apron as a tsunami-like surge as shown in Figure 6(c)-(d). A more in-depth discussion of the hydrodynamics can be found in Nistor et al. (2016).

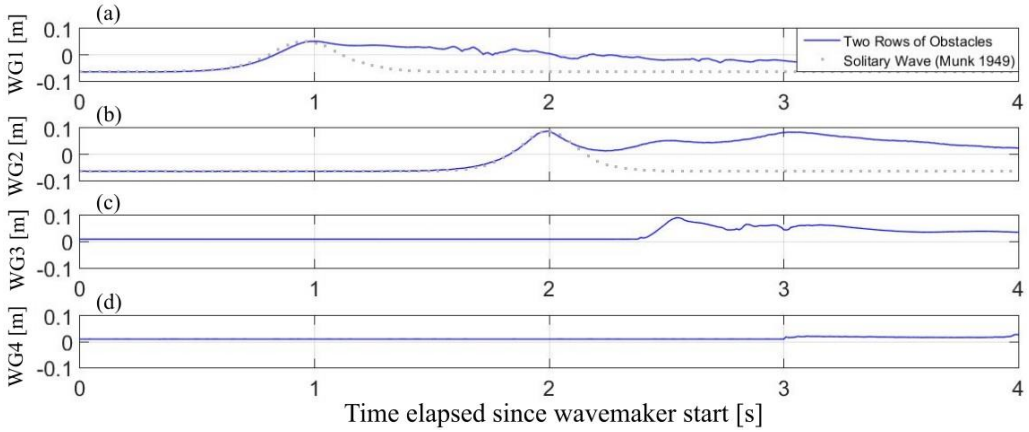

Figure 6: Time-history of water surface elevation at the four wave gages (WG) shown in Figure 1. The solitary wave profile is compared to the analytical solution by Munk (1949)

4.2 Debris Trajectory and Velocity

The trajectory of the debris was tracked by continuously monitoring the centroid of each debris throughout the AOI. With the centroid of each debris and the time stamp of each frame evaluated, the velocity of the debris could be further determined. In the evaluation of forces - later discussed in in Section 4.3 -the on-shore velocity (y-direction) was the component of interest as the structure perpendicular to the flow direction would experience maximum impact forces. Alternatively, as can be observed in Figure 7 and Figure 8, there is minimal motion in the cross-shore (x-direction) direction and minimal velocity. Due to this analysis, the velocity from herein on will only refer to the on-shore (y-direction) velocity. The orientation of the debris was determined by tracking the movement of the long axis of the debris.

As shown in Figure 7(a)-(b) and Figure 8(a)-(b), the trajectory of the debris with one and three debris was repeatable. The only case where there was significant deviation occurred when grounding of the one debris was observed in experiment #7. As debris propagated over the horizontal apron, likely due to the random nature of the turbulence of the incoming surge, the debris briefly contacts the apron resulting in a sharp deceleration at around 0.8 s (as shown in Figure 7(c)). As the debris propagated significantly slower than the surge, water built up on sides of the debris causing the debris to rotate towards the longer axis of the debris perpendicular to the flow direction. As the debris was rotating, the flow continued to act along the long axis resulting in the debris being pushed in the negative x-direction.

Unlike the trajectory, the orientation of the debris was significantly less repeatable. Overall, the debris tended to propagate in the same orientation as the initial position for each test for the length of the acceleration of the debris. However, as the debris decelerated as the debris fell out of the surge front, debris tended to orient perpendicular to the flow. As the debris slowed and the water surface elevation decreased, the debris contacted the horizontal apron resulting in periodic grounding similar to the more extreme case seen in experiment #7. Due to the random nature of

the periodic grounding caused by the turbulent surge front, the orientation tends to display a similar pattern but with significant variation between the tests.

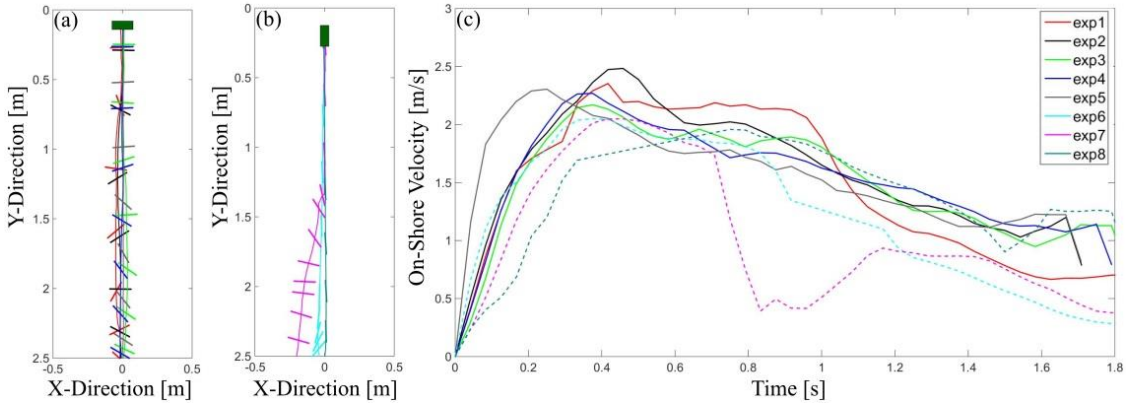

Figure 7: Motion and velocity of one debris. (a) the trajectory and orientation for E01; (b) the trajectory and orientation for E02; and (c) the on-shore (y-direction) velocity for E01 (solid line) and E02 (dashed line).

The velocity of the debris, as shown in Figure 7(c) and Figure 8(c), was also repeatable. For both the experiments with one and three debris, the debris oriented perpendicular to the flow reached a higher peak velocity. The debris velocities were between 6-14% higher than in the case of the experiments where debris were initially oriented parallel to the flow. The higher velocity was a result of the debris located perpendicular to the flow experiencing a greater drag force acting on the face of the debris, as the exposed cross-sectional area was larger (drag force is a function of cross-sectional area), resulting in larger accelerations (Imamura et al., 2008). However, once the debris had reached peak velocity, their subsequent deceleration was similar, regardless of their initial orientation of the debris.

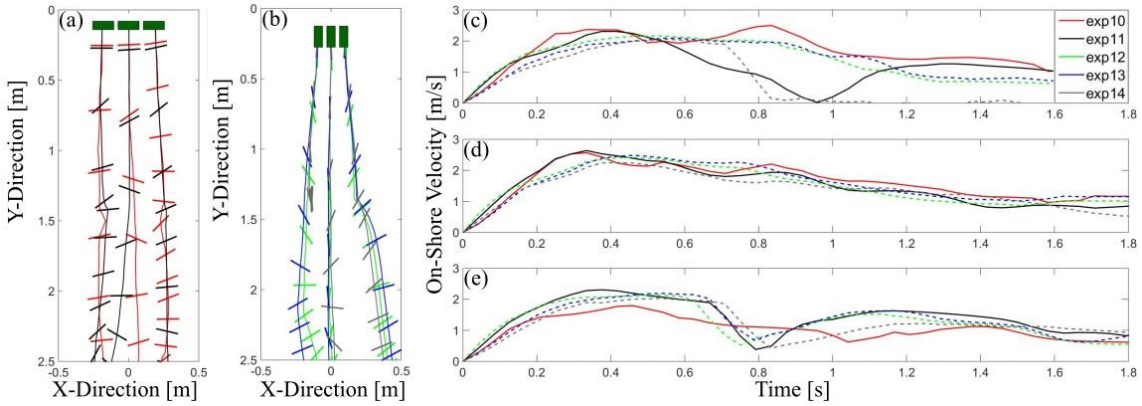

Figure 8. Motion and velocity of three debris. (a) trajectory and orientation for E03; (b) trajectory and orientation for E04; and (c) on-shore (y-direction) velocity for E03 (solid line) and E04 (dotted line) for D1 (c), D2 (d), and D3 (e).

The grounding of the debris had no noticeable effects on their velocity after the debris had been re-entrained within the flow. The debris that briefly grounded quickly returned to similar velocities to those of the debris that had not grounded. As debris grounded, water built up behind them causing a wake around the debris with little water present in front of the debris. When the debris was released, the hydraulic head difference (gradient) between the front and back of the debris resulted in subsequent sharp acceleration, which returned the debris to the velocity of debris that did not ground.

4.3 Debris Impact Force

Current (*FEMA P646, 2008*) and upcoming (*ASCE 7: Tsunami Loads and Effects, 2016*) design standard for debris impact in extreme hydrodynamic flows rely exclusively on incoming velocity of debris for calculating the impact

force. The equations used in the calculation of the forces are based on a simplified 1D bar model for the debris (Haehnel and Daly, 2004, Aghl et al., 2015):

[1] $F = u\sqrt{m_d k}$

where F is the impact force, u is the debris velocity at impact, m_d is the mass of the debris, and k is the lesser of the debris stiffness and the lateral stiffness of the impacted structural element. If the impacted structural element was not known, the stiffness was calculated using the elastic Young's modulus ($E = 1.9x10^9\ Pa$) of the debris material (Polyethylene) using:

[2] $k = \frac{EA}{L}$

where A is the cross-sectional area of the debris, and L is the long-axis of the debris. Previous work in debris impact testing indicated that maximum debris impact force occurred when the long-axis of the debris was perpendicular to the structure (Matskevitch, 1997, Haehnel and Daly, 2004, Aghl et al., 2015). The orientation of the impact would also significantly affect the impact force, however due to the highly random nature of the debris orientation, the maximum potential force was considered here.

Figure 9(a) compares debris velocities of all four experimental categories discussed. For the experiments with three debris, the peak velocities of the debris are up to 9% greater than the experiments with one debris. As the flow reaches the debris initially, there is little debris movement, thus causing the water to build up behind the debris. As the debris continued to remain stationary, water would continue to build up until the friction between the debris and the horizontal bottom was overcome. The built up water entrained and accelerated the debris within the flow propagating over the horizontal apron. This phenomena occurred for both experimental with one and three debris; however, due to more debris causing a larger blockage, the build up behind the three debris was increased. The result was greater acceleration and therefore higher peak velocities for the three debris experiments.

Figure 9(b)-(c) shows the potential debris impact force based on equation [1] for one and three debris as a function of dimensionless space (Y), where y is the displacement in the flow direction and L is the length of the debris. Along the flow transect, the debris underwent a rapid increase in potential impact force near the debris site. From $Y = 2$ to $Y = 10$, the impact force plateaus until the debris began to decelerate and the impact forces significantly lowered. Based on these conditions, the near-field structure would be of most concern for debris impact as the impact forces would be significantly larger.

The debris reached a maximum potential force earlier when the debris was initially oriented perpendicular to the flow for both one and three debris. However, for the case of three debris, the peak forces occur closer to the aprons edge comparing to the case with one debris. As discussed earlier, the three debris accelerated faster as a result of the water build up behind the debris on initial impact with the surge, resulting in larger accelerations and therefore reaching peak velocities earlier than in the case with one debris.

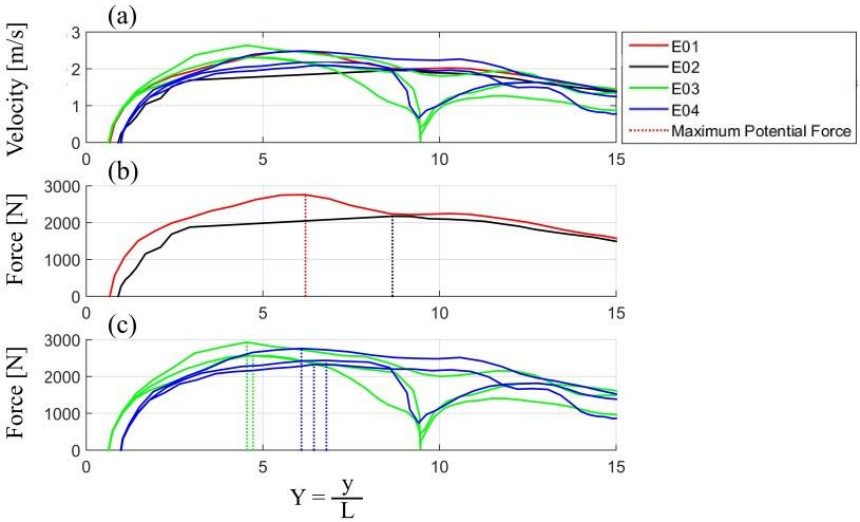

Figure 9: Impact forces due to debris propagates over the horizontal apron. (a) On-shore velocity for all groups; (b) and (c) Potential force over the apron from Aghl et al. (2015) for E01, E02 (b), E03, and E04(c) - dotted lines denote where the maximum force occurs.

5. SUMMARY AND CONCLUSIONS

This paper presents an analysis of debris motion using a novel, camera-based, optical tracking algorithm of experiments performed at Waseda University, Tokyo, Japan by the authors. The algorithm used multiple image processing techniques to quickly and accurately track the trajectory and orientation of the debris through the AOI. The experiments were run with one and three scaled-down shipping containers, orientated perpendicular or parallel to the flow direction, in an experimental setting mimicking a modern port environment. From this analysis, the following conclusions can be drawn:

- The repetitions of the experimental tests showed that the trajectory, as well as the velocity of the debris are consistent throughout all tests.
- Peak velocities of the debris oriented perpendicular to the flow direction occur earlier in time than the peak velocities of the debris oriented parallel to the flow.
- Peak velocities were greater when the debris was oriented perpendicular to the flow.
- Peak velocities of the experiments with three debris were larger than those observed during the experiments performed with one debris.
- Debris tended to orient towards the long axis perpendicular to the flow direction, regardless of their initial orientation.

While the work presented herein presents a brief analysis and explanation of the motion of debris, a more in-depth, detailed experiment with more experimental runs would allow for a probabilistic approach to better understand the phenomena involved. The analysis of the force of the debris on a structure would also help in the verification of the potential forces determined from these experiments.

ACKNOWLEDGMENTS

The authors gratefully acknowledge the access to the new Tsunami Wave Basin provided by colleagues at Waseda University in Tokyo, Japan. N. Goseberg acknowledges that this research was supported by a Marie Curie International Outgoing Fellowship within the 7th European Community Framework Program. I. Nistor acknowledges that this research was supported by the Kajima Foundation, Japan and the NSERC Discovery Grant.

REFERENCES

Aghl, P.P., Naito, C., Riggs, H., 2015. Estimation of demands resulting from inelastic axial impact of steel debris. *Engineering Structures* 82, 11–21.

Chai, D., Bouzerdoum, A., 2000. A Bayesian approach to skin color classification in YCbCr color space, *in: TENCON2000.Proceedings*. IEEE, pp. 421–424.

Clague, J.J., Munro, A., Murty, T., 2003. Tsunami hazard and risk in Canada. *Natural Hazards* 28, 435–463.

Esteban, M., Takagi, H., Shibayama, T., 2015. Handbook of Coastal Disaster Mitigation for Engineers and Planners.

Fujii, Y., Satake, K., Sakai, S., Shinohara, M., Kanazawa, T., 2011. Tsunami source of the 2011 off the Pacific coast of Tohoku Earthquake. *Earth, planets and space* 63, 815–820.

Goseberg, N., Nistor, I., Mikami, T., Shibayama, T., Stolle, J., 2015. Non-invasive Spatio-temporal "smart" debris Tracking in Turbulent Flows with Application to debris-laden Tsunami Inundation. In Review (Journal of Hydraulic Engineering).

Haehnel, R.B., Daly, S.F., 2004. Maximum impact force of woody debris on floodplain structures. *Journal of Hydraulic Engineering* 130, 112–120.

Harrabi, R., Braiek, E., 2011. Color image segmentation using automatic thresholding techniques, *in: Systems,Signals Devices (SSD), 2011 8th International Multi-Conference*. IEEE, pp. 1–6.

Imamura, F., Goto, K., Ohkubo, S., 2008. A numerical model for the transport of a boulder by tsunami. *Journal of Geophysical Research: Oceans (1978–2012)* 113.

Johnston, D., Paton, D., Crawford, G.L., Ronan, K., Houghton, B., Bürgelt, P., 2005. Measuring tsunami preparedness in coastal Washington, United States, *in: DevelopingTsunamiResilientCommunities*. Springer, pp. 173–184.

Kazama, M., Noda, T., 2012. Damage statistics (Summary of the 2011 off the Pacific Coast of Tohoku Earthquake damage). *Soils and Foundations* 52, 780–792.

Laplante, P.A., Neill, C.J., 2003. A class of Kalman filters for real-time image processing, *in: ElectronicImaging2003*. International Society for Optics and Photonics, pp. 22–29.

Madsen, P.A., Fuhrman, D.R., Schäffer, H.A., 2008. On the solitary wave paradigm for tsunamis. *Journal of Geophysical Research: Oceans* 113.

Matskevitch, D., 1997. Eccentric impact of an ice feature: linearized model. *Cold regions science and technology* 25, 159–171.

Matsutomi, H., 2009. Method for estimating collision force of driftwood accompanying tsunami inundation flow. *Journal of Disaster Research* 4, 435–440.

Matsutomi, H., Fujii, M., Yamaguchi, T., 2008. Experiments and development of a model on the inundated flow with floating bodies. *Coastal Engineering* 1458–1470.

Munk, W.H., 1949. The Solitary Wave Theory and Its Application to Surf Problems. *Annals of the New York Academy of Sciences* 51, 376–424.

Munkres, J., 1957. Algorithms for the assignment and transportation problems. *Journal of the Society for Industrial & Applied Mathematics* 5, 32–38.

Naito, C., Cercone, C., Riggs, H.R., Cox, D., 2014. Procedure for site assessment of the potential for tsunami debris impact. *Journal of Waterway, Port, Coastal and Ocean Engineering* 140, 223–232.

Nistor, I., Goseberg, N., Mikami, T., Shibayama, T., Stolle, J., Nakamura, R., Matsuba, S., 2016. Hydraulic Experiments on Debris Dynamics over a Horizontal Plane. In Review (Journal of Waterway, Port, Coastal, and Ocean Engineering).

Palermo, D., Nistor, I., Nouri, Y., Cornett, A., 2009. Tsunami loading of near-shoreline structures: a primer. *Canadian Journal of Civil Engineering* 36, 1804–1815.

Rueben, M., Cox, D., Holman, R., Shin, S., Stanley, J., 2014. Optical Measurements of Tsunami Inundation and Debris Movement in a Large-Scale Wave Basin. *Journal of Waterway, Port, Coastal, and Ocean Engineering* 141.

Salvi, G., 2012. An Automated Vehicle Counting System Based on Blob Analysis for Traffic Surveillance, *in: Proceedings International ConferenceImageProcessing,ComputerVision, Pattern Recognition (IPCV)*. The Steering Committee of The World Congress in Computer Science, Computer Engineering and Applied Computing (WorldComp), p. 1.

Shafiei, S., Melville, B., Beskhyroun, S., Shamseldin, A., 2014. Preliminary investigation of the tsunami-borne debris impact on structures: a new method for impact force measurement, *in: 5thIAHRInternationalSymposium Hydraulic Structures*. The University of Queensland, pp. 1–9.

Stolle, J., Nistor, I., Goseberg, N., 2016. Optical Tracking of Floating Shipping Containers in High-Velocity Flow. In Review (Coastal Engineering Journal).

Taubenböck, H., Goseberg, N., Lämmel, G., Setiadi, N., Schlurmann, T., Nagel, K., Siegert, F., Birkmann, J., Traub, K.-P., Dech, S., others, 2013. Risk reduction at the “Last-Mile”: an attempt to turn science into action by the example of Padang, Indonesia. *Natural hazards* 65, 915–945.

Taubenböck, H., Goseberg, N., Setiadi, N., Lämmel, G., Moder, F., Oczipka, M., Klüpfel, H., Wahl, R., Schlurmann, T., Strunz, G., others, 2009. Last-Mile" preparation for a potential disaster–Interdisciplinary approach towards tsunami early warning and an evacuation information system for the coastal city of Padang, Indonesia. *Natural Hazards and Earth System Science* 9, 1509–1528.

Yao, Y., Huang, Z., Lo, E.Y.M., Shen, H.-T., 2014. A preliminary laboratory study of motion of floating debris generated by solitary waves running up a beach. *Journal of Earthquake and Tsunami* 8.

Yeh, H., Sato, S., Tajima, Y., 2013. The 11 March 2011 East Japan earthquake and tsunami: tsunami effects on coastal infrastructure and buildings. *Pure and Applied Geophysics* 170, 1019–1031.